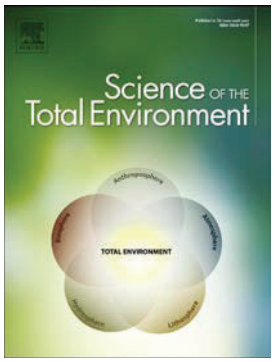

Toxic mechanisms of cigarette smoke and heat-not-burn tobacco vapor inhalation on rheumatoid arthritis

Cintia Scucuglia Heluany, Pablo Scharf, Ayda Henriques Schneider, Paula Barbim Donate, Walter dos Reis Pedreira Filho, Tiago Franco de Oliveira, Fernando Queiroz Cunha, Sandra Helena Poliselli Farsky

PII: S0048-9697(21)06175-1

DOI: https://doi.org/10.1016/j.scitotenv.2021.151097

Reference: STOTEN 151097

To appear in: *Science of the Total Environment*

Received date: 12 August 2021

Revised date: 24 September 2021

Accepted date: 16 October 2021

Please cite this article as: C.S. Heluany, P. Scharf, A.H. Schneider, et al., Toxic mechanisms of cigarette smoke and heat-not-burn tobacco vapor inhalation on rheumatoid arthritis, *Science of the Total Environment* (2021), https://doi.org/10.1016/j.scitotenv.2021.151097

Toxic mechanisms of cigarette smoke and heat-not-burn tobacco vapor inhalation on rheumatoid arthritis

Cintia Scucuglia Heluany[1#], Pablo Scharf[1#], Ayda Henriques Schneider[2], Paula Barbim Donate[2], Walter dos Reis Pedreira Filho[3], Tiago Franco de Oliveira[4], Fernando Queiroz Cunha[2], Sandra Helena Poliselli Farsky[1*]

[1] Department of Clinical & Toxicological Analyses, School of Pharmaceutical Sciences, University of Sao Paulo, SP, Brazil

[2] Department of Pharmacology, Ribeirao Preto Medical School, University of Sao Paulo

[3] Jorge Duprat Figueiredo Foundation for Occupational Safety and Medicine, Ministry of Economy, Sao Paulo, SP, Brazil

[4] Department of Pharmacosciences, Federal University of Health Sciences of Porto Alegre, Porto Alegre, RS, Brazil

# Both co-authors contributed equally.

*Corresponding author: Sandra Helena Poliselli Farsky

Department of Clinical and Toxicological Analyses School of Pharmaceutical Sciences University of São Paulo

Av. Prof. Lineu Prestes 580 Bl.13 B - Butantan, São Paulo, Brazil ZIP Code: 05508-900 Phone: 55-11-3091-1193

E-mail: sfarsky@usp.br

Abstract

Tobacco combustion exposure worsens rheumatoid arthritis (RA). Non-combustible tobacco devices, as heat-not-burn tobacco (HNBT), are emerging as harm reduction to smokers by releasing nicotine and lower combustible tobacco products. Nevertheless, HNBT toxicity remains unclear. Hence, here we investigated the impacts of the tobacco combustible product (cigarette smoke; CS) or HNBT vapor exposures on antigen-induced arthritis (AIA) in C57BL/6 mice. Animals were exposed to airflow, HNBT vapor, or CS during 1 hour/twice a day, under the Health Canada Intense (HCI) smoking regime, between days 14 to 20 after the first immunization. At day 21, 16h after the last exposures, mice were i.a. challenged and the AIA effects were evaluated 24h later. CS- or HNBT-exposed mice presented equivalent blood nicotine levels. CS exposure worsened articular symptoms, pulmonary inflammation, and expression of lung metallothioneins. Nevertheless, CS or HNBT exposures reduced lymphoid organs' cellularity, splenocyte proliferation and IL-2 secretion. Additional *in vitro* CS or HNBT exposures confirmed the harmful effects on splenocytes, which were partially mediated by the activation of nicotine/α7nAchR pathway. Associated, data demonstrate the toxic mechanisms of CS or HNBT inhalation at HCI regime on RA, and highlight that further investigations are fundamental to assure the toxicity of emerging tobacco products on the immune system during specific challenges.

Keywords: heat-not-burn tobacco; Nicotine; antigen-induced arthritis; splenocyte proliferation; α7 nicotinic acetylcholine receptor; IL-2; Health Canada Intense smoking regime

1. Introduction

Autoimmune diseases arise from an abnormal immune response against self-antigens, resulted from the immune tolerance breakdown. Rheumatoid arthritis (RA) is a chronic autoimmune disease manifested by inflammatory polyarthritis, especially in the small joints, resulting in joints destruction and bone erosion which leads to deformity and disability (McInnes and Schett, 2011). The symptoms occur due to an intense influx of inflammatory cells into the joints combined with enhanced proliferation of synoviocytes, which are responsible to secrete soluble mediators to perpetuate the inflammation and to produce reactive oxygen (ROS) and nitrogen species (RNS) that damage the tissues (Huber et al., 2006). Moreover, RA events are also accompanied by systemic extra-articular manifestations, such as lung and cardiovascular complications (Solomon et al., 2006; Olson et al., 2011).

RA prevalence is 0.5-1% in the world population, with a higher impact especially on women and aged people (Tobon et al., 2009; Ngo et al., 2014). The genesis of RA outcomes is influenced by genetic predisposition, exposure to environmental factors and lifestyle (Karami et al., 2019). In this context, the incidence of RA is higher in industrialized countries, showing that the exposure of humans to environmental pollutants is involved in the onset and progression of the disease (Sigaux et al., 2019). Among the known environmental risk factors associated with RA in humans, cigarette smoking is by far the most significant. Cigarette smoke (CS) exposure has been correlated with the increased incidence, worsening of RA, and reduced therapy responsiveness in humans (Firestein 2003, Klareskog et al., 2006; Giuseppe et al., 2014; Ishikawa et al., 2019).

CS is a complex aerosol system composed of roughly 8,700 identified substances (Stabbert et al., 2017). The toxic action of tobacco combustible products on RA, including polycyclic aromatic hydrocarbon (PAH) or benzene metabolites, is mainly attributed to the activation of the aryl hydrocarbon receptor (AhR; Kobayashi et al., 2008; Talbot et al., 2018; Heluany et al., 2018a, b; Heluany et al., 2021). AhR is a cytosolic transcription factor activated by environmental pollutants, which is essential for the differentiation and activation of pathogenic T helper (Th) 17 lymphocytes during the RA genesis (Nguyen et al., 2015). Moreover, the activation of oxidative stress by CS compounds is a potential mechanism involved in the RA, as ROS mediate a diversity of intracellular

pathways of immune activation (Mateen et al., 2016; Phull et al., 2018). Indeed, toxic CS products, such as benzene and its metabolites, metals, and PAH, activate membrane and mitochondrial pathways of ROS production (Sklorz et al., 2007; Barreiro et al., 2010; Heluany et al., 2018b; Fabris et al., 2020).

Meanwhile robust evidence suggests the role of combustible tobacco products on RA genesis, the participation of nicotine in the disease course still controversial. Studies carried out in experimental animals exposed to nicotine by oral, intravenous, subcutaneous, or intraperitoneal routes outcome controversial data (van Maanen et al., 2009; Lindblad et al., 2009; Li et al., 2017; Wu et al., 2014; Yu et al., 2011; Yang et al., 2014; Wasén et al., 2017; Lee et al., 2017; Goldbarari et al., 2019). It has been proposed that nicotine displays anti-inflammatory effects by interacting with the α7 nicotinic acetylcholine receptor (α7nAchR) on immune cells (Wang et al., 2003; Revathikumar et al., 2016). The suggested anti-inflammatory mechanisms involve the activation of the suppressor of cytokine signaling 3 (SOCS-3), inhibition of NFκB translocation into nucleus in inflamed synoviocytes (Yoshikawa et al., 2006; Zhou et al., 2012; Li et al., 2017), or the polarization of Th2 rather than Th17 lymphocytes (Wu et al., 2014; 2018). Conversely, it was demonstrated that nicotine administration worsened collagen-induced arthritis (CIA) in mice, displaying higher levels of neutrophil-extracellular trap (NET)-associated myeloperoxidase (MPO)-DNA complex on the plasma of the exposed-animals. Furthermore, incubation of human neutrophils with nicotine led to a dose-dependent NET formation, which was abrogated by pre-incubation with an antagonist of α7nAch receptor (Lee et al., 2017).

Concerning the deleterious effects of CS and tobacco combustion exposure to humans, efforts have been made for the development of alternative ways of nicotine delivery (Callahan-Lyon et al., 2014; Hampson et al., 2015). Indeed, non-combustible cigarette devices have emerged as promising tools for harm reduction compared to conventional cigarettes, such as electronic cigarettes and heat-not-burn tobacco products (HNBT) (St. Helen et al., 2018; Zhao et al., 2018). HNBT devices heat tobacco but do not burn it, thus reducing the release of products from tobacco combustion and delivering mainly nicotine, propylene glycol, and glycerin (Forster et al., 2018; Dusautoir et al., 2020). Hence, amounts of toxic combustible products are markedly reduced, while it is claimed that the amounts of nicotine are equivalent to those found in conventional cigarettes (Mallock et al., 2018). Although clinical and

experimental studies have grown up in recent years, data obtained are so far away to describe the real toxicity of alternative pathways of tobacco exposures.

To address the role of tobacco products on RA development, we here compared the effects of two nicotine-content tobacco products (CS or HNBT vapor) exposures by inhalation route on the local and systemic symptoms of antigen-induced arthritis (AIA) in mice. The exposures of CS or HNBT were carried out under the Health Canada Intense (HCI) smoking regime and were adjusted to obtain equivalent serum nicotine as achieved in moderate-heavy smokers. Data obtained showed that only CS exposure aggravated AIA symptoms. Nevertheless, both CS and HNBT exposures reduced the cellularity on lymphoid tissues, which may be due the impairment of IL-2 dependent proliferation caused by nicotine delivered by such CS as HNBT vapor exposure.

2. Material and Methods

2.1 Animals

Adult male C57BL/6 mice (8-weeks old) were housed in an animal facility at the School of Medicine of Ribeirão Preto, University of São Paulo, with controlled temperature and light conditions and were supplemented with food and water *ad libitum*. Animal husbandry and all procedures were in accordance with the guidelines of the Animal Ethics Committee of the School of Medicine of Ribeirão Preto, University of Sao Paulo (protocol number 048/2012).

2.2 In vivo exposures

Mice were exposed to airflow, CS from conventional filter-tipped cigarettes (Marlboro Red, Phillip Morris), or HNBT vapor (IQOS heatsticks, Phillip Morris International) under the Health Canada Intense (HCI) smoking regime (55mL of smoke for 2 seconds puffing, for every 30 seconds). For such, an exposure machine was designed (Bonther, Brazil), allowing simultaneous exposures of the three experimental groups, with controlled humidity, temperature, and constant air exhausting to avoid mice intoxication. CS and HNBT vapor generated by the heatsticks were aspirated by a vacuum pump and delivered to the exposure chambers. The number of cigarettes and heatsticks used were matched

by the amount of nicotine released and by the absorption and metabolism of the compound by the animals. For each hour of exposure, 12 conventional cigarettes and 24 heatsticks were used. Animals were daily exposed (1 hour/ twice a day; 9-10 AM and 3-4 PM) to air, CS or HNBT during 7 consecutive days after the second immunization (between days 14 to 20). The exposure machine and the experimental design are shown in the Suppl. Fig. 1.

2.3 Antigen-induced arthritis (AIA)

AIA was induced as previously described by Schneider et al. (2020) and Heluany et al. (2021).

2.3.1 Measurement of mechanical articular hyperalgesia and edema

The articular hyperalgesia and edema formation were measured as previously described by Heluany et al. (2021). Briefly, hyperalgesia assessment was performed 24 hours after and before local mBSA challenge, by applying perpendicular force to the central area of the plantar surface of the hind paw to induce flexion of the femur-tibial joint followed by the paw withdrawal. The mechanical threshold was expressed in grams (g), whereas the hyperalgesia was calculated to the reduction of this threshold. The edema formation in the right knee joints was determined in the femur-tibial joint area, using a caliper, before and 24 hours after the i.a. mBSA challenge. The edema unit was expressed in millimeters (mm) through the quantification of paw volumes.

2.3.2 Samples harvest, cell counting and characterization

Twenty-four hours after the mBSA challenge, mice were euthanized and the blood, synovial fluid, spleen, and the popliteal draining lymph nodes (DLNs) were collected, processed and the number of cells was determined through cell counting on a Neubauer chamber with a light microscope. Results were expressed as the number of cells x 10^6 per sample. For the *ex-vivo* stimulation, 2 x 10^6 splenocytes were plated in RPMI culture medium supplemented with 10 % FBS and stimulated with phorbol-myristate acetate (PMA; 50 nM; Sigma-Aldrich) and ionomycin (500 ng/mL; Invitrogen) for 24 hours. After that, the supernatants were collected and stored at -70°C until used to quantify cytokines levels by ELISA. The synovial fluid was obtained through 2 injections of 10 µL of

phosphate-buffer saline (PBS) in the femur-tibial articular cavities. Cells were diluted in Turk´s solution and their total number was determined through cell counting on Neubauer chamber. Results were expressed as the number of cells per joint.

2.3.3 Neutrophil extracellular traps (NETs) quantification

NETs concentration was assessed as previously described (Schneider et al. 2020) by the quantification of myeloperoxidase (MPO)-DNA complexes in the synovial fluid. Results were expressed as nanograms (ng) of NETs produced per milliliter (mL) of sample.

2.3.4 Quantification of cytokines levels

Concentration of the secreted monocyte chemoattractant protein-1 (MCP-1) was quantified in the synovial fluid collected from all the exposed-AIA groups, using a CBA mouse kit according to the manufacturer´s specifications (BD Pharmingen). Concentrations of IL-2 and IL-10 on *ex-vivo* and *in vitro* stimulated splenocytes were quantified using commercial ELISA mouse kits according to the manufacturer's specifications (BD Opteia). Results were expressed as picograms (pg) of cytokine produced per milliliter (mL) of fluid or supernatant.

2.3.5 Histopathological analysis and lung inflammation scoring

Twenty-four hours after the mBSA challenge, the lungs were collected and fixed in 4% paraformaldehyde for 24 hours without positive tracheal pressure, dehydrated in graded ethanol, cleared in xylene, and embedded in paraffin for histopathological and immunohistochemical analyses. The sections (4µm) were stained with hematoxylin and eosin and analyzed using 20x or 40x magnification objective lenses, using an optical microscope (Zeiss microscope; Carl Zeiss. For the histopathological analyses, three sections/lung were microscopically evaluated and scored in a blinded manner and seven fields per slide were considered for analysis. The inflammation scores indicated the averages of the scores for the number of infiltrating inflammatory cells and intra-alveolar macrophage aggregates; and alveolar wall thickness. All scores were relative scores on a grade scale from 0-4, with zero representing healthy lung, without inflammatory alterations; 1 representing minimal change; 2

representing mild change; 3 representing moderate change; and 4 representing marked change, with the results, expressed as the mean inflammation score, as previously described by Matute-Bello et al., 2011. Data were expressed as arbitrary units.

2.3.6 Immunohistochemistry

The detection of hepatic and pulmonary metallothioneins (MTs) was performed by immunohistochemistry as previously described (Scharf et al., 2021). The tissue sections were incubated with anti-metallothionein 1/2 (ABCAM) overnight at 4°C, and further incubated with a secondary antibody conjugated with HRP (ABCAM) for 1 hour at RT. The staining was detected with DAB substrate (DAKO). The sections were counterstained with hematoxylin and mounted with a non-aqueous Entellan mounting media (Sigma-Aldrich). The relative mean of intensity of DAB staining was determined in an arbitrary scale ranging from 0 to 255 in the free software ImageJ (National Institute of Health, USA). For such, 7 fields per slide were photographed using a 40× highpower objective and the mean of intensity was generated.

2.4 Quantification of metals levels

The levels of metals after the exposures were quantified in the exposure chambers by inductively coupled plasma mass spectrometry (ICP-MS; Agilent Technologies). Briefly, ester-cellulose membrane filters with 0.8 µm porosity and 37 mm diameter (Millipore) were placed in the exposure chambers and exposed to the airflow, CS or HNBT, for 1 hour, according to the exposure protocol described above. Then, the filters were carefully removed and digested using a microwave oven (MARS 6) followed by an acid digestion method. After that, 5 mL of ultrapure water (MilliQ) and 5 mL of HNO3 (Sigma-Aldrich) were added to vessels containing the exposed filters for 25 minutes (15 minutes at ramp stage and 10 minutes on hold at 180 ºC). Then, 5 mL of ultrapure water was added, and the levels of the metals nickel (Ni), chromium (Cr), aluminum (Al) and cooper (Cu) were quantified via ICP-MS. Results were presented as microgram (µg) of metal generated per liter (L).

2.5 Nicotine and cotinine measurements

Nicotine and cotinine levels were quantified in the plasma collected from naïve C57BL/6 mice exposed for 1 hour to airflow, HNBT vapor or CS. At the end of exposures, blood was collected by cardiac puncture in heparinized tubes for plasma obtainment. An aliquot of 15 µL of an acetonitrile/methanol solution (80:20, v/v) was added to the plasma (20 µL/sample) spiked with 5 µL of the internal standard (testosterore-d_3; 1 µg/mL). After centrifugation for 10 minutes at 9000 *g* an aliquot of 10 µL was injected into the UHPLC-ESI-MS/MS system for quantification of nicotine and cotinine using a Nexera UFLC system coupled to a LCMS-8040 triple quadrupole mass spectrometer (Shimadzu, Japan). For data evaluation, LabSolutions software (Shimadzu, Japan) was used to obtain the peak areas for each exposed group.

2.6 In vitro exposure system and protocol

The *in vitro* exposures to CS, HNBT vapor, airflow or nicotine were performed as previously described (Scharf et al., 2021). Briefly, cells were placed on 12 mm transwell inserts (0.4 µm porosity; Corning, USA) at the density of $1x10^6$ cells/per well and exposed to air, or 4 conventional cigarettes (Marlboro Red, Philip Morris) or to 5/6 heatsticks of the HNBT device (IQOS; Philip Morris International) in acrylic exposure chambers. The protocol exposure consisted of a 2-second cycle of exposure to CS or HNBT vapor (at 45 rpm) followed by 58 seconds of air (at 25 rpm), for 30 minutes. A continuous flow of serum-free culture medium was maintained at 20 rpm.

2.7 AhR expression

AhR expression was assessed 2 hours after the splenocytes *in vitro* exposures by flow cytometry as previously described (Heluany et al., 2021). Harvested splenocytes were fixed and permeabilized with CytoPerm/CytoFix kit (BD Biosciences) and incubated with anti-AhR primary antibody (1:100, ABCAM) for 1 hour at RT. After washing, cells were incubated with a secondary antibody conjugated with Alexa Fluor 647 (1:250, ABCAM) for 1 hour at RT. Data were obtained in an Accuri C6 flow cytometer (BD Biosciences), by recording 10,000 events. Results are presented as the fold change in relation to arbitrary units of fluorescence from the basal group.

2.8 Th17 polarization assay

$CD4^+$ T cells were purified from spleen and lymph nodes isolated from naïve C57BL/6 male mice using an anti-$CD4^+$ microbeads cocktail, according to the manufacturer instructions (Miltenyi Biotech). The $CD4^+$ cells purity was assessed by flow cytometry before the exposures and only $CD4^+$ cell population ranging from 90-95 % of purity were considered for the further experiments. After isolation, $CD4^+$ cells ($1x10^6$ cells/well) were exposed to the air, CS, HNBT or nicotine as described above and cultured under Th17 polarization conditions with anti-CD3 and anti-CD28 (2 µg/mL, plate-bound, and 2 µg/ml, soluble, respectively, ABCAM), rmTGF-β1 (2.5 ng/mL), and rmIL-6 (25 ng/mL, both BD Biosciences) for 72 hours. Before the flow cytometry analysis, cells were stimulated with PMA (50 nM; Sigma-Aldrich) and ionomycin (500 ng/mL; Invitrogen) for 4 hours. Then, the samples were fixed and permeabilized with CytoPerm/CytoFix kit (BD Biosciences), washed once with PBS, and incubated with anti-IL17A-PE and anti-CD4-FICT (both 1:50; BD Biosciences) for 1 hour at RT. After the washing step, 10,000 events were recorded in an Accuri C6 flow cytometer (BD Biosciences) and data were expressed as percentual of $CD4^+/IL17^+$ cells.

2.9 Proliferation assay

Splenocytes isolated from naïve C57BL/6 mice ($1x10^6$ cells/well) were stained with carboxyfluorescein succinimidyl ester (2 µM; CFSE, Invitrogen) and incubated for 15 minutes at 37 ºC, washed twice with PBS and were exposed to airflow, HNBT vapor or CS or treated 30 minutes with nicotine (0.01 µM; 0.1 µM or 1 µM, Sigma-Aldrich), and further stimulated with Concanavalin A (ConA; 10 ng/mL, Sigma-Aldrich). To assess the role of α7nAchR activation on splenocyte proliferation, the CFSE-labeled splenocytes were pre-incubated for 1 hour at 37 ºC with the inversible antagonist of α7nAchR, α-bungarotoxin (200 nM; α-BTX, Invitrogen) or vehicle (PBS) and exposed to air, HNBT vapor, CS or nicotine as described above. Thus, the cell proliferation was monitored for 72 hours, and 30,000 events were recorded in an Accuri C6 flow cytometer (BD Biosciences). Data were expressed as the percentage of proliferative cells.

2.10 Reactive oxygen species (ROS) detection

The intracellular accumulation of reactive oxygen species (ROS) was determined in splenocyte cultures using the fluorescent probe CellRox Deep Red (Molecular Probes). The measurement was carried out immediately after exposures following the procedures described by Scharf et al. (2021) and Heleuany et al. (2021). Data obtained in 10,000 events were acquired in an Accuri C6 cytometer (BD Biosciences). Data were expressed as the fold change in relation to MFI signal from ROS production from the basal group.

2.11 Data analysis

Statistical analyses were performed using one-way analysis of variance (ANOVA), followed by *post hoc* comparisons using the Tukey test. The values are presented as mean ± standard error of the mean (S.E.M.) and the level of significance adopted was 95 % ($p < 0.05$). Analyses were performed using GraphPad Prism version 7.0 (GraphPad Software, USA).

3. Results and Discussion

3.1 Levels of nicotine and cotinine in exposed mice

It has been claimed that HNBT devices deliver significantly smaller levels of combustible products and similar amounts of nicotine into exposed subjects than CS (Schaller et al., 2016; Auer et al., 2017; Mallock et al., 2018). This assumption was first validated in our experimental approach, as the literature data related to nicotine exposures on RA are still controversial, and data were obtained in exposures conditions which do not reflect smokers' exposure. Hence, we investigated local and systemic symptoms of RA under equivalent levels of plasma nicotine and cotinine in CS- or HNBT-exposed animals submitted to the Health Canada Intense (HCI) smoking regime, which provided pulse-controlled exposure of CS or HNBT vapor as occurs in smokers (Fig. 1A, B).

3.2 Levels of metals in the chamber

Heavy metals are known toxic agents that trigger inflammation and oxidative stress (Kocadal et al., 2020). Whilst reduced levels of combustible tobacco products have been fully characterized in HNBT vapors using similar approach of in vivo exposure employed in the present study (Auer et al., 2017),

lower levels of heavy metals by HNBT device was only showed in an in vitro system of cell exposure (Scharf et al., 2021). Here we confirmed that HNBT device released lower levels of Cr, Al and Ni than CS into the in vivo exposure chambers. Values of these metals in the HNBT chamber were similar to those obtained in the air-exposed group and lower than those found in the CS chamber (Fig. 1C-E); meanwhile levels of Cu were not even detectable in the airflow or HNBT-exposed groups (Fig. 1F).

3.3 Effects of CS or HNBT exposures on local and systemic AIA symptoms

Although RA is a complex, multifactorial and chronic disease, AIA is a T-cell driven experimental model and a versatile tool for examining several parameters and mechanisms related to RA symptoms, such as hypernociception, edema formation, joint inflammation, T cell behavior, neutrophil influx, and NETs formation (Brand, 2005; van den Berg et al., 2007, Schneider et al., 2021). Using this experimental model, we showed that CS exposure before the AIA challenge caused more intense hypernociception (Fig. 2A) and edema in the knee joints (Fig. 2B), increased the influx of inflammatory cells, mainly neutrophils (Fig. 2C), augmented the NETs production (Fig. 2D) and enhanced MCP-1 levels (Fig. 2E) in the synovial fluid of the exposed-mice in comparison to HNBT or airflow exposures.

Pulmonary disease is an extra-articular manifestation which contributes to cause morbidity and mortality in patients with RA (Bongartz et al., 2010, Bernstein et al., 2016). Herein, such CS or HNBT exposures into AIA-mice increased the lung inflammation; nevertheless, the lesion in the lungs was more severe in CS exposed animals (Fig. 3A-E), characterized by intense inflammatory cell infiltrate and loss of intra-alveolar spaces related to interstitial lung inflammation and alveolar wall thickness (Fig. 3F). It is worth to mention that although mice under AIA and exposed to HNBT vapor showed no statistical difference in comparison to the CS group, HNBT vapor exposures lead to a low-grade lung inflammation similar to airflow-exposed mice but higher than the naive group.

Metallothioneins (MTs) are scavenger of metals and ROS, and therefore they are overexpressed upon metal intoxications and inflammatory conditions (Ruttkay-Nedecky et al., 2013; Juaréz-Rebollar et al., 2017). Here we showed that the CS exposure marked augmented the MTs expression in the lungs in relation to expressions evoked by airflow or HNBT vapor exposures (Fig. 3F-J). Hence, we

infer that the systemic inflammatory and oxidative stress caused by CS exposure may be also accounted due to the higher levels of heavy metals delivered during tobacco combustion, which also triggers MTs expression as a mechanism to counterbalance the aggression into tissues evoked CS exposure.

Associated, data obtained here corroborated the role of combustible tobacco products content in the CS worsening local and systemic inflammatory symptoms of RA (Kobayashi et al., 2008; Nguyen et al., 2015; Talbot et al. 2018; Heluany et al., 2018a, b; Heluany et al., 2021), and also pointed out novel phenomena of systemic tobacco exposure by airways and elucidate controversial data of the literature, as follow i) higher levels of metals delivered by CS into lungs trigger host defense mechanisms, which is not enough to halt lung damage in CS-exposed mice; ii) HNBT exposure following controlled HCI smoking regime does not cause prominent lung inflammation as it has been claimed by the literature; iii) nicotine content in the HNBT vapor absorbed by airway route as employed by smokers does not significantly inhibit the inflammatory effects on RA.

*3.*4 CS or HNBT exposures reduce the cellularity in the lymphoid tissues in AIA-mice

Inflamed peripheral tissues and lymph nodes operate as a functional unit in chronic inflammation, by the effective cross talk and reciprocal modulation on trafficking of immune cells and inflammatory chemical mediators, on tissue immune surveillance and on maintenance of peripheral tolerance (Bouta et al., 2018). Hence, we also assessed the total cellularity of spleen and draining lymph nodes (DLNs) as a parameter of disease activity and systemic inflammation. Surprisingly, either CS or HNBT exposures during the last phase of AIA markedly reduced the cellularity of lymphoid organs in comparison to airflow-exposed group (Fig. 4A, B). Marked impairment on lymphocyte number in draining lymph nodes were also obtained in CS- and HNBT-exposed mice during the development of collagen-induced arthritis, which did not reflect augmented cell death in the lymphoid tissues (Heluany, personal communication). Therefore, it may be supposed that CS or HNBT exposures during AIA led to the impairment of cell trafficking, proliferation and activation in the lymphoid tissues, and these hypotheses were further elucidated using splenocytes isolated from AIA mice

exposed to airflow, CS or HNBT or splenocytes obtained from naïve mice and further i*n vitro* exposed to xenobiotics.

3.5 In vitro CS exposure leads to AhR expression, Th17 polarization and oxidative burst in splenocytes

AhR activation in leukocytes, especially $CD4^+$ T lymphocytes, is a pivotal mechanism involved in the genesis of RA, and a supposed effector in the worsening of the disease after environmental factor exposures, such as cigarette smoking (Nguyen et al., 2013; Kishimoto et al., 2015). Here we show that splenocytes exposed to CS produced higher levels of ROS than those exposed to HNBT vapor or airflow in response to PMA (Fig. 5A). Furthermore, only the CS exposure increased the expression of AhR (Fig. 5B) and switched $CD4^+$ cells into Th17 cell profile (Fig. 5C). It is noteworthy to mention that i*n vitro* exposures to airflow or HNBT vapor did not enhance cell death in comparison to non-exposed cells, and that CS exposure slightly reduced the viability of the cell suspension, mainly due to causing necrosis (Suppl. Fig. 2). Recent data have depicted the mechanisms involved in the AhR activation and Th17 polarization. It was shown that the CS exposure causes the generation of miRNA related to Th17 lymphocyte polarization through AhR activation (Donate et al., 2020), and the administration of an AhR agonist into mice carrying human SE-coding alleles resulted in augmented symptoms of RA and IL17-expressing cells in the inflamed joints and draining lymph nodes of arthritic mice (Fu et al., 2018). Therefore, the data herein presented corroborate the fundamental role of combustible tobacco products in the AhR/IL-17 pathway on worsening of RA (Nguyen et al, 2013; Talbot et al., 2018; Heluany et al., 2018b, Heluany et al., 2021), and show, for the first time, the HNBT exposure does not trigger these inflammatory mechanisms involved on RA development.

3.6 CS and HNBT vapor exposures impair splenocyte proliferation and IL-2 secretion partially through the α7nAchR activation

Splenocytes isolated from CS- or HNBT-exposed mice and further stimulated with PMA/ionomycin secreted lower levels of IL-2 and higher levels of IL-10 compared with cells obtained from air-exposed mice (Fig. 4C, D). IL-2 acts as a growth factor leading to the proliferation of activated T cells, and is a pivotal cytokine involved in immune surveillance and tolerance (Amado et

al., 2013; Ward et al., 2018). IL-10 is a potent anti-inflammatory mediator, which suppresses T cell proliferation and inhibits IL-2 secretion by activated T cells (Fitzgerald et al., 2007; Schülke, 2018). Therefore, we suppose the imbalance of the cytokines in lymphoid tissues is a plausible toxic mechanism of tobacco products which could impair the proliferation of splenocytes. Indeed, *in vitro* exposures to CS or HNBT vapor decreased ConA-induced splenocyte proliferation. The HNBT-exposed group displayed a more intense impairment on cell proliferation rate when compared to cells exposed to CS (Fig. 6A, B). As acute or long-term exposures to nicotine impair *in vivo* and *in vitro* lymphocyte proliferation (Singh et al., 2000; Kalra et al., 2000), herein we further confirmed that nicotine exposure also reduced the proliferation rate of naïve splenocytes (Fig. 6A, B).

Nicotine binds to a class of membrane nicotinic acetylcholine receptors (nAChRs) widespread in different tissues, and several isoforms of nAChRs are expressed in immune cells (Qian et al., 2011; Fujii et al., 2017; Gomes et al., 2018). The subunit α-7nAChRs is involved in regulating T cell proliferation and differentiation, cytokine secretion, and antigen presentation of immune cells in either innate or adaptive immunity (Martelli et al., 2014; Fujii et al., 2017; Mashimo et al., 2019). Hence, we further investigated how the α-7nAchR blockage could modulate the splenocyte proliferation under CS, HNBT or nicotine exposures. Thus, we showed that splenocytes pre-treated with α-BTX, an α-7nAChR antagonist, and further exposed to CS, HNBT vapor or nicotine were able to rescue the cell proliferation (Fig. 6A, B). Furthermore, CS, HNBT or nicotine exposures impaired the secretion of IL-2, which levels were rescued if cells were previously treated with α-7nAChR (Fig. 6C-E). These data confirm the involvement of the IL-2 on toxicity of tobacco products on splenocytes, mainly induced by the nicotine binding to α-7nAchR. The non-completely recovery of splenocytes proliferation and IL-2 secretion by blocking α7-nAchR could be explained by the fact that other nAChRs subunits are expressed on lymphocytic cells, such as α4, α9 and, α10 subunit, which could also mediate the nicotine effects (Qian et al. 2011; Fujii et al. 2017; Gomes et al. 2018).

Conclusion

The data herein presented show different toxic mechanisms of tobacco delivery devices during the development of RA. The worsening of inflammatory symptomatology of AIA evidenced the toxicity

caused by inhalation of combustible products of tobacco, and CS or HNBT inhalation highlighted the toxicity of both xenobiotic on lymphoid tissues during AIA development, which may be accounted by the nicotine immunosuppressive actions. The impairment on T cell biology caused by HNBT vapor or CS exposure may be involved on other smoke-related diseases, such as cancer immune scape and invasiveness. Hence, further well-delineated experimental studies are required to establish the real toxicity of CS and the recent commercialized HNBT devices on the activation of immune cells and their outcomes in tobacco addicts.

Declaration of Competing Interest

The authors declare that the research was conducted in the absence of any commercial or financial relationships that could be construed as a potential conflict of interest.

Authorship contribution statement

CSH: Conceptualization, data collection, analyses, interpretation and manuscript writing, revision and proof-read. **PS**: Conceptualization, data collection, analyses, interpretation and manuscript writing, revision and proof-read. **AHS**: Data collection, manuscript proof-read. **PBD**: Data collection, manuscript proof-read. **WRPF**: Data collection, manuscript proof-read. **TFO**: Data collection, manuscript proof-read. **FQC**: Data collection, interpretation, manuscript writing and revision and proof-read. **SHPF**: Conceptualization, supervision, interpretation and manuscript writing, revision and proof-read.

Acknowledgements

The authors thank the Fundação de Amparo à Pesquisa do Estado de São Paulo (FAPESP; S.H.P.F. - research grant 2019/19573-7, and research grant 2013/08216-2 Center of Research on Inflammatory Diseases) for providing post-doctoral fellow to C.S.H. (grant number 2017/26998-9), and the Conselho Nacional de Desenvolvimento Científico e Tecnológico (CNPq) for providing Master fellow to P. S. (grant number 130090/2019-0) and Researcher fellow to F. Q. C. and S. H. P. F.

References

Amado, I. F., Berges, J., Luther, R. J., Mailhé, M.-P., Garcia, S., Bandeira, A., Weaver, C., Liston, A., Freitas, A. A., 2013. IL-2 coordinates IL-2–producing and regulatory T cell interplay. J. Exp. Med. 210(12), 2707–2720. https://doi.org/10.1084/jem.20122759.

Auer, R., Concha-Lozano, N., Jacot-Sadowski, I., Cornuz, J., Berthet, A., 2017. Heat-Not-Burn Tobacco Cigarettes. JAMA Int. Med. 177(7), 1050. https://doi.org/10.1001/jamainternmed.2017.1419.

Barreiro, E., Peinado, V. I., Galdiz, J. B., Ferrer, E., Marin-Corral, J., Sánchez, F., Gea, J., Barberà, J. A., 2010. Cigarette Smoke–induced Oxidative Stress. Am. J. Respir. Crit. Care Med. 182(4), 477–488. https://doi.org/10.1164/rccm.200908-1220oc.

Bernstein, E. J., Barr, R. G., Austin, J. H. M., Kawut, S. M., Raghu, G., Sell, J. L., Hoffman, E. A., Newell, J. D., Jr, Watts, J. R., Jr, Nath, P. H., Sonavane, S. K., Dathon, J. M., Majka, D. S., Lederer, D. J., 2016. Rheumatoid arthritis-associated autoantibodies and subclinical interstitial lung disease: the Multi-Ethnic Study of Atherosclerosis. Thorax 71(12), 1082–1090. https://doi.org/10.1136/thoraxjnl-2016-208932.

Bongartz, T., Nannini, C., Medina-Velasquez, Y. F., Achenbach, S. J., Crowson, C. S., Ryu, J. H., Vassallo, R., Gabriel, S. E., Matteson, E. L., 2010. Incidence and mortality of interstitial lung disease in rheumatoid arthritis: A population-based study. Arthritis Rheum. 62(6), 1583–1591. https://doi.org/10.1002/art.27405.

Bouta, E. M., Bell, R. D., Rahimi, H., Xing, L., Wood, R. W., Bingham, C. O., Ritchlin, C. T., Schwarz, E. M., 2018. Targeting lymphatic function as a novel therapeutic intervention for rheumatoid arthritis. Nat. Rev. Rheum. 14(2), 94–106. https://doi.org/10.1038/nrrheum.2017.205.

Brand, D. D., 2005. Rodent models of rheumatoid arthritis. Comp. Med. 55, 114-122.

Callahan-Lyon, P., 2014. Electronic cigarettes: human health effects. Tob. Control 23(suppl 2), ii36–ii40. https://doi.org/10.1136/tobaccocontrol-2013-051470.

Donate, P. B., Alves de Lima, K., Peres, R. S., Almeida, F., Fukada, S. Y., Silva, T. A., Nascimento, D. C., Cecilio, N. T., Talbot, J., Oliveira, R. D., Passos, G. A., Alves-Filho, J. C., Cunha, T. M., Louzada-Junior, P., Liew, F. Y., Cunha, F. Q., 2020. Cigarette smoke induces miR-132in Th17 cells that enhance osteoclastogenesis in inflammatory arthritis. Proc. Natl. Acad. Sci. U.S.A. 118(1), e2017120118. https://doi.org/10.1073/pnas.2017120118.

Dusautoir, R., Zarcone, G., Verriele, M., Garçon, G., Fronval, I., Beauval, N., Allorge, D., Riffault, V., Locoge, N., Lo-Guidice, J.-M., Anthérieu, S., 2020. Comparison of the chemical composition of aerosols from heated tobacco products, electronic cigarettes and tobacco cigarettes and their toxic impacts on the human bronchial epithelial BEAS-2B cells. J. Hazard. Mater. 401, 123417. https://doi.org/10.1016/j.jhazmat.2020.123417.

Fabris, A. L., Nunes, A. V., Schuch, V., de Paula-Silva, M., Rocha, G., Nakaya, H. I., Ho, P. L., Silveira, E. L. V., Farsky, S. H. P., 2020. Hydroquinone exposure alters the morphology of lymphoid organs in vaccinated C57Bl/6 mice. Environ. Pollut. 257, 113554. https://doi.org/10.1016/j.envpol.2019.113554.

Firestein, G. S., 2003. Evolving concepts of rheumatoid arthritis. Nature 423(6937), 356–361. https://doi.org/10.1038/nature01661.

Fitzgerald, D. C., Zhang, G.-X., El-Behi, M., Fonseca-Kelly, Z., Li, H., Yu, S., Saris, C. J. M., Gran, B., Ciric, B., Rostami, A. 2007. Suppression of autoimmune inflammation of the central nervous system by interleukin 10 secreted by interleukin 27–stimulated T cells. Nature Immunol. 8(12), 1372–1379. https://doi.org/10.1038/ni1540.

Forster, M., Fiebelkorn, S., Yurteri, C., Mariner, D., Liu, C., Wright, C., McAdam, K., Murphy, J., Proctor, C., 2018. Assessment of novel tobacco heating product THP1.0. Part 3: Comprehensive chemical characterisation of harmful and potentially harmful aerosol emissions. Regul. Toxicol. Pharmacol. 93, 14-33. https://doi.org/10.1016/j.yrtph.2017.10.006.

Fu, J., Nogueira, S. V., Drongelen, V. van, Coit, P., Ling, S., Rosloniec, E. F., Sawalha, A. H., Holoshitz, J., 2018. Shared epitope–aryl hydrocarbon receptor crosstalk underlies the mechanism of gene–environment interaction in autoimmune arthritis. Proc. Natl. Acad. Sci. U.S.A. 115(18), 4755–4760. https://doi.org/10.1073/pnas.1722124115.

Fujii, T., Mashimo, M., Moriwaki, Y., Misawa, H., Ono, S., Horiguchi, K., Kawashima, K., 2017. Expression and Function of the Cholinergic System in Immune Cells. Front. Immunol. 8. https://doi.org/10.3389/fimmu.2017.01085.

Gahring, L. C., Myers, E. J., Rogers, S. W., 2020. Inhaled aerosolized nicotine suppresses the lung eosinophilic response to house dust mite allergen. Am. J. Physiol. Lung Cell Mol. Physiol. 319(4), L683–L692. https://doi.org/10.1152/ajplung.00227.2020.

Giuseppe, D., Discacciati, A., Orsini, N., Wolk, A., 2014. Cigarette smoking and risk of rheumatoid arthritis: a dose-response meta-analysis. Arthritis Res. Ther. 16(2), R61. https://doi.org/10.1186/ar4498.

Golbahari, S., Abtahi Froushani, S. M., 2019. Synergistic benefits of Nicotine and Thymol in alleviating experimental rheumatoid arthritis. Life Sciences 239, 117037. https://doi.org/10.1016/j.lfs.2019.117037.

Gomes, J. P., Watad, A., Shoenfeld, Y., 2018. Nicotine and autoimmunity: The lotus' flower in tobacco. Pharmacol. Res. 128, 101-109. https://doi:10.1016/j.phr.2017.10.005.

Hampson, S. E., Andrews, J. A., Severson, H. H., Barckley, M., 2015. Prospective Predictors of Novel Tobacco and Nicotine Product Use in Emerging Adulthood. J. Adolesc. Health 57(2), 186–191. https://doi.org/10.1016/j.jadohealth.2015.04.015.

Heluany, C. S., Kupa, L. de V. K., Viana, M. N., Fernandes, C. M., Farsky, S. H. P., 2018a. Hydroquinone exposure worsens the symptomatology of rheumatoid arthritis. Chem. –Biol. Interact. 291, 120–127. https://doi.org/10.1016/j.cbi.2018.06.016.

Heluany, C. S., Kupa, L. de V. K., Viana, M. N., Fernandes, C. M., Silveira, E. L. V., Farsky, S. H. P., 2018b. In vivo exposure to hydroquinone during the early phase of collagen-induced arthritis aggravates the disease. Toxicology 408, 22–30. https://doi.org/10.1016/j.tox.2018.06.010.

Heluany, C. S., Donate, P. B., Schneider, A. H., Fabris, A. L., Gomes, R. A., Villas-Boas, I. M., Tambourgi, D. V., Silva, T. A., Grossini, G. H. G., Nalesso, G., Silveira, E. L. V., Cunha, F. Q., Farsky, S. H. P. 2021. Hydroquinone Exposure Worsens Rheumatoid Arthritis through the Activation of the Aryl Hydrocarbon Receptor and Interleukin-17 Pathways. Antioxidants 10(6), 929. https://doi.org/10.3390/antiox10060929.

Hosseinzadeh, A., Thompson, P. R., Segal, B. H., Urban, C. F., 2016. Nicotine induces neutrophil extracellular traps. J. Leuk. Biol. 100(5), 1105–1112. https://doi.org/10.1189/jlb.3ab0815-379rr.

Huber, L. C., Distler, O., Tarner, I., Gay, R. E., Gay, S., Pap, T., 2006. Synovial fibroblasts: key players in rheumatoid arthritis. Rheumatology 45(6), 669–675. https://doi.org/10.1093/rheumatology/kel065.

Ishikawa, Y., Ikari, K., Hashimoto, M., Ohmura, K., Tanaka, M., Ito, H., Taniguchi, A., Yamanaka, H., Mimori, T., Terao, C., 2019. Shared epitope defines distinct associations of cigarette smoking with levels of anticitrullinated protein antibody and rheumatoid factor. Ann. Rheum. Dis. 78(11), 1480–1487. https://doi.org/10.1136/annrheumdis-2019-215463.

Juárez-Rebollar, D., Rios, C., Nava-Ruíz, C., Méndez-Armenta, M., 2017. Metallothionein in Brain Disorders. Oxid. Med. Cell Longev. 2017, 1–12. https://doi.org/10.1155/2017/5828056.

Kalra, R., Sigh, S. P., Savage, S. M., Fich, G. L., Sopori, M. L., 2000. Effects of cigarette smoke on immune response: chronic exposure to cigarette smoke impairs antigen-mediated signaling in T cells and depletes IP3-sensitive Ca(2+) stores. J. Pharmacol. Exp. Ther. 293 (1) 166-171.

Karami, J., Aslani, S., Jamshidi, A., Garshasbi, M., Mahmoudi, M., 2019. Genetic implications in the pathogenesis of rheumatoid arthritis; an updated review. Gene 702, 8–16. https://doi.org/10.1016/j.gene.2019.03.033.

Kishimoto, T., Nguyen, N. T., Nakahama, T., Nguyen, H. C., Tran, T. T., Le, V. S., Chu, H. H., 2015. Aryl hydrocarbon receptor antagonism and its role in rheumatoid arthritis. J. Exp. Med. 29. https://doi.org/10.2147/jep.s63549.

Klareskog, L., Stolt, P., Lundberg, K., Kallberg, H., Bengtsson, C., Grunewald, J., Rönnelid, J., Erlandsson Harris, H., Ulfgren, A.-K., Rantapää-Dahlqvist, S., Eklund, A., Padyukov, L., Alfredsson, L., 2005. A new model for an etiology of rheumatoid arthritis: Smoking may trigger HLA–DR (shared epitope)–restricted immune reactions to autoantigens modified by citrullination. Arthritis Rheum. 54(1), 38–46. https://doi.org/10.1002/art.21575.

Kobayashi, S., Okamoto, H., Iwamoto, T., Toyama, Y., Tomatsu, T., Yamanaka, H., Momohara, S., 2008. A role for the aryl hydrocarbon receptor and the dioxin TCDD in rheumatoid arthritis. Rheumatology 47(9), 1317–1322. https://doi.org/10.1093/rheumatology/ken259.

Kocadal, K., Alkas, F., Battal, D., Saygi, S., 2019. Cellular pathologies and genotoxic effects arising secondary to heavy metal exposure: A review. Hum. Exp. Toxicol. 39(1), 3–13. https://doi.org/10.1177/0960327119874439.

Lee, J., Luria, A., Rhodes, C., Raghu, H., Lingampalli, N., Sharpe, O., Rada, B., Sohn, D. H., Robinson, W. H., Sokolove, J., 2017. Nicotine drives neutrophil extracellular traps formation and

accelerates collagen-induced arthritis. Rheumatology 56, 644-653. https://doi.org/10.1093/rheumatology/kew449.

Li, T., Wu, S., Li, S., Bai, X., Luo, H., Zuo, X., 2017. SOCS3 participates in cholinergic pathway regulation of synovitis in rheumatoid arthritis. Connect. Tissue Res. 1–8. https://doi.org/10.1080/03008207.2017.1380633.

Lindblad, S. S., Mydel, P., Jonsson, I.-M., Senior, R. M., Tarkowski, A., Bokarewa, M., 2009. Smoking and nicotine exposure delay development of collagen-induced arthritis in mice. Arthritis Res. Ther. 11(3), R88. https://doi.org/10.1186/ar2728.

Mallock, N., Pieper, E., Hutzler, C., Henkler-Stephani, F., Luch, A., 2019. Heated Tobacco Products: A Review of Current Knowledge and Initial Assessments. Front. Public Health, 7. https://doi.org/10.3389/fpubh.2019.00287.

Martelli, D., McKinley, M. J., McAllen, R. M., 2014. The cholinergic anti-inflammatory pathway: A critical review. Auton. Neurosci. 182, 65–69. https://doi.org/10.1016/j.autneu.2013.12.007.

Mashimo, M., Komori, M., Matsui, Y. Y., Murase, M. X., Fujii, T., Takeshima, S., Okuyama, H., Ono, S., Moriwaki, Y., Misawa, H., Kawashima, K., 2019. Distinct Roles of α7 nAChRs in Antigen-Presenting Cells and CD4+ T Cells in the Regulation of T Cell Differentiation. Front. Immunol. 10. https://doi.org/10.3389/fimmu.2019.01102.

Matute-Bello, G., Downey, G., Moore, B. B., Groshong, S. D., Matthay, M. A., Slutsky, A. S., Kuebler, W. M., 2011. An Official American Thoracic Society Workshop Report: Features and Measurements of Experimental Acute Lung Injury in Animals. Am. J. Respir. Cell Mol. Biol. 44(5), 725–738. https://doi.org/10.1165/rcmb.2009-0210st.

Mateen, S., Moin, S., Khan, A. Q., Zafar, A., Fatima, N., 2016. Increased Reactive Oxygen Species Formation and Oxidative Stress in Rheumatoid Arthritis. PLOS ONE, 11(4), e0152925. https://doi:10.1371/journal.pone.0152925.

McInnes, I. B., Schett, G., 2011. The Pathogenesis of Rheumatoid Arthritis. N. Engl. J. Med. 365(23), 2205–2219. https://doi.org/10.1056/nejmra1004965.

Ngo, S. T., Steyn, F. J., McCombe, P. A., 2014. Gender differences in autoimmune disease. Front. Neuroendrocinol. 35(3), 347–369. https://doi.org/10.1016/j.yfrne.2014.04.004.

Nguyen, N. T., Nakahama, T., Kishimoto, T., 2013. Aryl hydrocarbon receptor and experimental autoimmune arthritis. Semin. Immunopathol. 35(6), 637–644. https://doi.org/10.1007/s00281-013-0392-6.

Nguyen, C. H., Nakahama, T., Dang, T. T., Chu, H. H., Van Hoang, L., Kishimoto, T., Nguyen, N. T., 2017. Expression of aryl hydrocarbon receptor, inflammatory cytokines, and incidence of rheumatoid arthritis in Vietnamese dioxin-exposed people. J. Immunotoxicol. 14(1), 196–203. https://doi.org/10.1080/1547691x.2017.1377323.

Olson, A. L., Swigris, J. J., Sprunger, D. B., Fischer, A., Fernandez-Perez, E. R., Solomon, J., Murphy, J., Cohen, M., Raghu, G., Brown, K. K., 2011. Rheumatoid Arthritis–Interstitial Lung Disease–associated Mortality. Am. J. Respir. Crit. Care Med. 183(3), 372–378. https://doi.org/10.1164/rccm.201004-0622oc.

Pinheiro, N. M., Santana, F. P. R., Almeida, R. R., Guerreiro, M., Martins, M. A., Caperuto, L. C., Câmara, N. O. S., Wensing, L. A., Prado, V. F., Tibério, I. F. L. C. Prado, M. A. M., Prado, C. M., 2016. Acute lung injury is reduced by the α7nAChR agonist PNU-282987 through changes in the macrophage profile. FASEB J. 31(1), 320–332. http://doi.org/10.1096/fj.201600431r.

Phull, A.-R., Nasir, B., Haq, I. ul, Kim, S. J., 2018. Oxidative stress, consequences and ROS mediated cellular signaling in rheumatoid arthritis. Chem. –Biol. Interact. 281, 121–136. https://doi.org/10.1016/j.cbi.2017.12.024.

Qian, J., Galitovskiy, V., Chernyavsky, A. I., Marchenko, S., Grando, S. A., 2011. Plasticity of the murine spleen T-cell cholinergic receptors and their role in in vitro differentiation of naïve CD4 T cells toward the Th1, Th2 and Th17 lineages. Genes Immun. 12(3), 222–230. https://doi.org/10.1038/gene.2010.72.

Revathikumar, P., Bergqvist, F., Gopalakrishnan, S., Korotkova, M., Jakobsson, P.-J., Lampa, J., Le Maître, E., 2016. Immunomodulatory effects of nicotine on interleukin 1β activated human astrocytes and the role of cyclooxygenase 2 in the underlying mechanism. J. Neuroinflammation 13(1). https://doi:10.1186/s12974-016-0725-1.

Riveiro-Naveira, R. R., Valcárcel-Ares, M. N., Almonte-Becerril, M., Vaamonde-García, C., Loureiro, J., Hermida-Carballo, L., López-Peláez, E., Blanco, F. J., López-Armada, M. J., 2016. Resveratrol lowers synovial hyperplasia, inflammatory markers and oxidative damage in an acute antigen-induced arthritis model. Rheumatology 55, 1889–1900. https://doi:10.1093/rheumatology/kew255.

Ruttkay-Nedecky, B., Nejdl, L., Gumulec, J., Zitka, O., Masarik, M., Eckschlager, T., Stiborova, M., Adam, V., Kizek, R., 2013. The Role of Metallothionein in Oxidative Stress. Int. J. Mol. Sci. 14, 6044–6066. https://doi.org/10.3390/ijms14036044.

Schaller, J.-P., Keller, D., Poget, L., Pratte, P., Kaelin, E., McHugh, D., Cudazzo, G., Smart, D., Tricker, A. R., Gautier, L., Yerly, M., Reis Pires, R., Le Bouhellec, S., Ghosh, D., Hofer, I., Garcia, E., Vanscheeuwijck, P., Maeder, S., 2016. Evaluation of the Tobacco Heating System 2.2. Part 2: Chemical composition, genotoxicity, cytotoxicity, and physical properties of the aerosol. Regul. Toxicol. Pharmacol. 81, S27–S47. https://doi.org/10.1016/j.yrtph.2016.10.001.

Scharf, P., da Rocha, G. H. O., Sandri, S., Heluany, C. S., Pedreira Filho, W. R., Farsky, S. H. P., 2021. Immunotoxic mechanisms of cigarette smoke and heat-not-burn tobacco vapor on Jurkat T cell functions. Environ. Pollut. 268, 115863. https://doi.org/10.1016/j.envpol.2020.115863.

Schneider, A. H., Machado, C. C., Veras, F. P., Maganin, A. G. de M., de Souza, F. F. L., Barroso, L. C., de Oliveira, R. D. R., Alves-Filho, J. C., Cunha, T. M., Fukada, S. Y., Louzada-Júnior, P., da Silva, T. A., Cunha, F. Q., 2020. Neutrophil extracellular traps mediate joint hyperalgesia induced by immune inflammation. Rheumatology. https://doi.org/10.1093/rheumatology/keaa794

Schülke, S., 2018. Induction of Interleukin-10 Producing Dendritic Cells As a Tool to Suppress Allergen-Specific T Helper 2 Responses. Front. Immunol. 9. https://doi.org/10.3389/fimmu.2018.00455.

Sigaux, J., Biton, J., André, E., Semerano, L., Boissier, M.-C., 2019. Air pollution as a determinant of rheumatoid arthritis. Joint Bone Spine 86(1), 37–42. https://doi.org/10.1016/j.jbspin.2018.03.001.

Singh, S. P., Kalra, R., Puttfarcken, P., Kozak, A., Tesfaigzi, J., Sopori, M. L., 2000. Acute and Chronic Nicotine Exposures Modulate the Immune System through Different Pathways. Toxicol. Appl. Pharmacol. 164(1), 65–72. https://doi.org/10.1006/taap.2000.8897.

Sklorz, M., Briedé, J.-J., Schnelle-Kreis, J., Liu, Y., Cyrys, J., de Kok, T. M., Zimmermann, R., 2007. Concentration of Oxygenated Polycyclic Aromatic Hydrocarbons and Oxygen Free Radical Formation from Urban Particulate Matter. J. Toxicol. Env. Heal. Part A. 70(21), 1866–1869. https://doi.org/10.1080/15287390701457654.

Solomon, D. H., Goodson, N. J., Katz, J. N., Weinblatt, M. E., Avorn, J., Setoguchi, S., Canning, C., Schneeweiss, S., 2006. Patterns of cardiovascular risk in rheumatoid arthritis. Ann. Rheum. Dis. 65, 1608–1612. https://doi:10.1136/ard.2005.050377.

St.Helen, G., Jacob III, P., Nardone, N., Benowitz, N. L., 2018. IQOS: examination of Philip Morris International's claim of reduced exposure. Tob. Control 27(Suppl 1), s30–s36. https://doi.org/10.1136/tobaccocontrol-2018-054321.

Stabbert, R., Dempsey, R., Diekmann, J., Euchenhofer, C., Hagemeister, T., Haussmann, H.-J., Knorr, A., Mueller, B. P., Pospisil, P., Reininghaus, W., Roemer, E., Tewes, F. J., Veltel, D. J., 2017. Studies on the contributions of smoke constituents, individually and in mixtures, in a range of in vitro bioactivity assays. Toxicol. In Vitro 42, 222-246. https://doi:10.1016/j.tiv.2017.04.003.

Talbot, J., Peres, R. S., Pinto, L. G., Oliveira, R. D. R., Lima, K. A., Donate, P. B., Silva, J. R., Ryffel, B., Cunha, T. M., Alves-Filho, J. C., Liew, F. Y., Louzada-Junior, P., Cunha, F. Q., 2018. Smoking-induced aggravation of experimental arthritis is dependent of aryl hydrocarbon receptor activation in Th17 cells. Arthritis Res. Ther. 20(1). https://doi.org/10.1186/s13075-018-1609-9.

Tobon, G. J., Youinou, P., Saraux, A., 2010. The environment, geo-epidemiology, and autoimmune disease: Rheumatoid arthritis. Autoimmun. Rev. 9(5), A288–A292. https://doi.org/10.1016/j.autrev.2009.11.019.

van den Berg, W. B., Joosten, L. A. B., van Lent, P. L. E. M., 2007. Murine Antigen-Induced Arthritis. Arthritis Res. 136, 243–253. Humana Press. https://doi.org/10.1007/978-1-59745-402-5_18.

van Maanen, M. A., Lebre, M. C., van der Poll, T., LaRosa, G. J., Elbaum, D., Vervoordeldonk, M. J., Tak, P. P., 2009. Stimulation of nicotinic acetylcholine receptors attenuates collagen-induced arthritis in mice. Arthritis Rheum. 60(1), 114–122. https://doi.org/10.1002/art.24177.

Ward, N. C., Yu, A., Moro, A., Ban, Y., Chen, X., Hsiung, S., Keegan, J., Arbanas, J. M., Loubeau, M., Thankappan, A., Yamniuk, A. P., Davis, J. H., Struthers, M., Malek, T. R., 2018. IL-2/CD25: A Long-Acting Fusion Protein That Promotes Immune Tolerance by Selectively Targeting the IL-2 Receptor on Regulatory T Cells. J. Immunol. 201(9), 2579–2592. https://doi.org/10.4049/jimmunol.1800907.

Wang, H., Yu, M., Ochani, M., Amella, C. A., Tanovic, M., Susarla, S., Li, J. H., Wang, H., Yang, H., Ulloa, L., Al-Abed, Y., Czura, C. J., Tracey, K. J., 2003. Nicotinic acetylcholine receptor α7 subunit is

an essential regulator of inflammation. Nature 421(6921), 384–388. https://doi.org/10.1038/nature01339.

Wasén, C., Turkkila, M., Bossios, A., Erlandsson, M., Andersson, K. M., Ekerljung, L., Malmhäll, C., Brisslert, M., Töyrä Silfverswärd, S., Lundbäck, B., Bokarewa, M. I., 2017. Smoking activates cytotoxic CD8+ T cells and causes survivin release in rheumatoid arthritis. J. Autoimmun. 78, 101–110. https://doi.org/10.1016/j.jaut.2016.12.009.

Wu, S., Luo, H., Xiao, X., Zhang, H., Li, T., & Zuo, X., 2014. Attenuation of collagen induced arthritis via suppression on Th17 response by activating cholinergic anti-inflammatory pathway with nicotine. Eur. J. Pharmacol. 735, 97–104. https://doi.org/10.1016/j.ejphar.2014.04.019.

Wu, S., Zhou, Y., Liu, S., Zhang, H., Luo, H., Zuo, X., Li, T., 2018. Regulatory effect of nicotine on the differentiation of Th1, Th2 and Th17 lymphocyte subsets in patients with rheumatoid arthritis. Eur. J. Pharmacol. 831. https://doi:10.1016/j.ejphar.2018.04.028.

Yang, Y., Yang, Y., Yang, J., Xie, R., Ren, Y., Fan, H., 2013. Regulatory effect of nicotine on collagen-induced arthritis and on the induction and function of in vitro-cultured Th17 cells. Modern Rheumatol. 24(5), 781–787. https://doi.org/10.3109/14397595.2013.862352.

Yoshikawa, H., Kurokawa, M., Ozaki, N., Nara, K., Atou, K., Takada, E., Kamochi, H., Suzuki, N., 2006. Nicotine inhibits the production of proinflammatory mediators in human monocytes by suppression of I-kappaB phosphorylation and nuclear factor-kappaB transcriptional activity through nicotinic acetylcholine receptor alpha7. Clin. Exp. Immunol. 146(1), 116–123. https://doi.org/10.1111/j.1365-2249.2006.03169.x.

Yu, H., Yang, Y.-H., Rajaiah, R., Moudgil, K. D., 2011. Nicotine-induced differential modulation of autoimmune arthritis in the Lewis rat involves changes in interleukin-17 and anti-cyclic citrullinated peptide antibodies. Arthritis Rheum. 63(4), 981–991. https://doi.org/10.1002/art.30219.

Zhao, J., Zhang, Y., Sisler, J. D., Shaffer, J., Leonard, S. S., Morris, A. M., Qian, Y., Bello, D., Demokritou, P., 2018. Assessment of reactive oxygen species generated by electronic cigarettes using acellular and cellular approaches. J. Hazard. Mater. 344, 549–557. https://doi.org/10.1016/j.jhazmat.2017.10.057.

Zhou, Y., Zuo, X., Li, Y., Wang, Y., Zhao, H., Xiao, X., 2010. Nicotine inhibits tumor necrosis factor-α induced IL-6 and IL-8 secretion in fibroblast-like synoviocytes from patients with rheumatoid arthritis. Rheumatol. Int. 32(1), 97–104. https://doi.org/10.1007/s00296-010-1549-4.

Figure Legends

Figure 1. Plasmatic levels of nicotine and cotinine and heavy metals delivered in the exposure chambers. Naïve C57BL/6 mice were exposed for 1 hour to airflow, CS and HNBT vapor, and immediately after exposures, plasma was collected to quantify nicotine (**A**) and cotinine (**B**) levels. For the quantification of heavy metals, ester cellulose filters were displayed on the exposures chambers and exposed for 1 hour for further quantification of nickel (**C**), chromium (**D**), aluminum (**E**), and copper (**F**). Data represent mean ± SEM of five animals/filters in each group and were analyzed by one-way ANOVA. (A-B) $^{*}p<0.05$ and $^{**}p<0.01$ versus air. No significant (ns) HNBT versus CS. (C-F) $^{\#\#}p<0.01$, $^{\#\#\#}p<0.001$ versus control. $^{\&}p<0.05$, $^{\&\&}p<0.01$ versus HNBT.

Figure 2. CS, but not HNBT vapor exposure, worsens AIA symptoms. C57BL/6 mice were exposed to airflow, HNBT vapor or to CS twice a day, 1 hour/exposure, between days 14-20 after the first immunization. On the day 21 after the first immunization, mice were i.a. challenged with mBSA. Twenty-four hours later, mechanical hyperalgesia (**A**) and edema (**B**) were assessed before mice euthanasia. After euthanasia, synovial fluid cellularity (**C**), concentration of NET formation (**D**), and MCP-1 secretion (**E**) on the synovial fluid were quantified. Data represent mean ± SEM of six animals/samples for each group and were analyzed by one-way ANOVA. $^{*}p<0.05$, $^{**}p<0.01$, $^{***}p<0.001$ versus naïve. $^{\#}p<0.05$, $^{\#\#\#}p<0.001$ versus air. $^{\&}p<0.05$, $^{\&\&\&}p<0.001$ versus HNBT.

Figure 3. CS leads to lung inflammation and increases the expression of metallothioneins. C57BL/6 mice were exposed to airflow, HNBT vapor or to CS twice a day, 1 hour/exposure, between days 14-20 after the first immunization. On the day 21 after the first immunization, mice were i.a. challenged with mBSA. Twenty-four hours later, mice were euthanized, and the lungs were collected to assess the histopathological score (**A-E**) and the expression of metallothionein I and II (MT I/II) by immunohistochemistry (**F-I**) and mean intensity of immunoreactive areas (**J**). Data represent mean ± SEM of five animals for each group and were analyzed by one-way ANOVA. $^{*}p<0.05$, $^{**}p<0.01$, $^{***}p<0.001$ *versus* Control/Naive. $^{\#\#}p<0.01$, $^{\#\#\#}p<0.001$ *versus* air. $^{\&}p<0.05$, $^{\&\&}p<0.01$ *versus* HNBT. Sections: 5 mm. (**A-D**) Arrowhead: inflammatory cell infiltration; Arrow: decreased intra-alveolar space. (**F-I**) Arrowhead: immunoreactive areas. Original magnification 20x.

Figure 4. CS or HNBT exposures reduce spleen and DLNs cellularity during AIA development and reduce the ex-vivo cytokine release by splenocytes. C57BL/6 mice were exposed to air, HNBT vapor or to CS twice a day, 1 hour/exposure, between days 14-20 after the first immunization. On the day 21 after the first immunization, mice were i.a. challenged with mBSA. Twenty-four hours later, mice were euthanized and inguinal DLNs (**A**) and spleens (**B**) were collected, processed, and their cellularitywere quantified. Splenocytes ($2x10^6$ cells/well) from naïve C57BL/6 mice were stimulated with PMA (50 nM) for 24 hours and the levels of IL-2 (**C**) and IL-10 (**D**) were quantified in the

supernatants through ELISA. Data represent mean ± SEM of six mice in each group and were analyzed by one-way ANOVA. $^{*}p<0.05$ versus naïve. $^{\#}p<0.05$, $^{\#\#}p<0.01$ versus air group.

Figure 5. CS exposure leads to oxidative burst, AhR activation and increased Th17 polarization. Splenocytes from naïve C57BL/6 mice ($1x10^6$ cells/well were exposed to air, HNBT vapor or CS. ROS production was quantified 30 minutes after the end of exposures, using a DCFH-DA assay (**A**). The AhR activation was assessed 2 hours after the end of the exposures through flow cytometry (**B**). $CD4^+$ naïve cells were exposed to air, HNBT vapor and CS, after exposures cultivate under Th17 polarization conditions for 72 hours (**C**). Data represent mean ± SEM of four mice in each group and were analyzed by one-way ANOVA. $^{*}p<0.05$, $^{**}p<0.01$, $^{***}p<0.01$ versus naïve. $^{\#}p<0.05$, $^{\#\#}p<0.01$, $^{\#\#\#}p<0.001$ versus air group. $^{\&\&\&}p<0.001$ versus HNBT group.

Figure 6. HNBT vapor, CS or nicotine exposure impairs the splenocyte proliferation and IL-2 secretion through α7AchR activation. Splenocytes from naïve C57BL/6 mice ($1x10^6$) were exposed to airflow, HNBT vapor, CS, or nicotine (0.01 μM, 0.1 μM or 1 μM). After that, the cell proliferation was monitored for 72 hours. CFSE-labeled splenocytes were stimulated with ConA (10ng/mL) and/or pre-treated with α-BTX (200 nM) or vehicle (PBS) 1 hour before the exposures. Representative histogram (**A**) and percentual (**B**) of proliferative cells. The splenocytes supernatants were collected to quantify the secreted levels of IL-2 after 24 hours (**C**), 48 hours (**D**), and 72 hours (**E**) of exposures. Data represent mean ± SEM of four mice in each group and were analyzed by one-way ANOVA. $^{***}p<0.001$ versus non-stimulated control group. $^{\#}p<0.05$, $^{\#\#\#}p<0.001$ versus Con-A stimulated control group. $^{\&}p<0.05$, $^{\&\&\&}p<0.001$ versus respective non-treated (α-BTX) group.

Figure 1

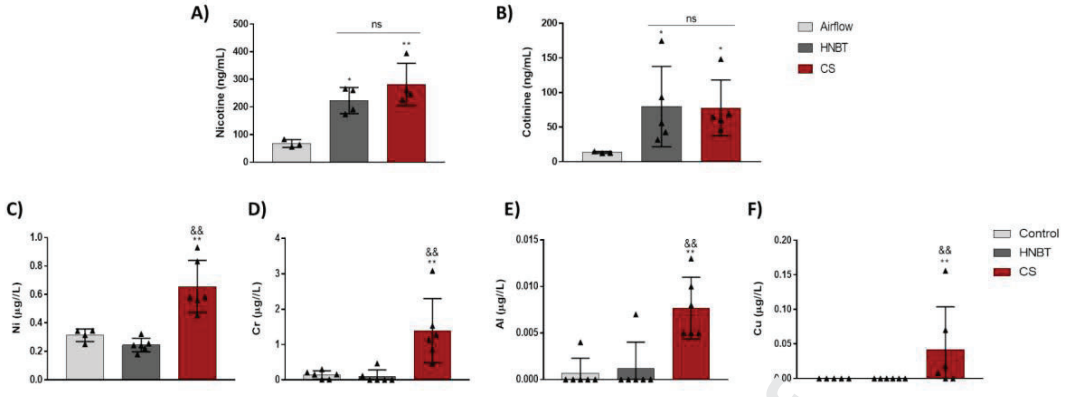

Figure 2

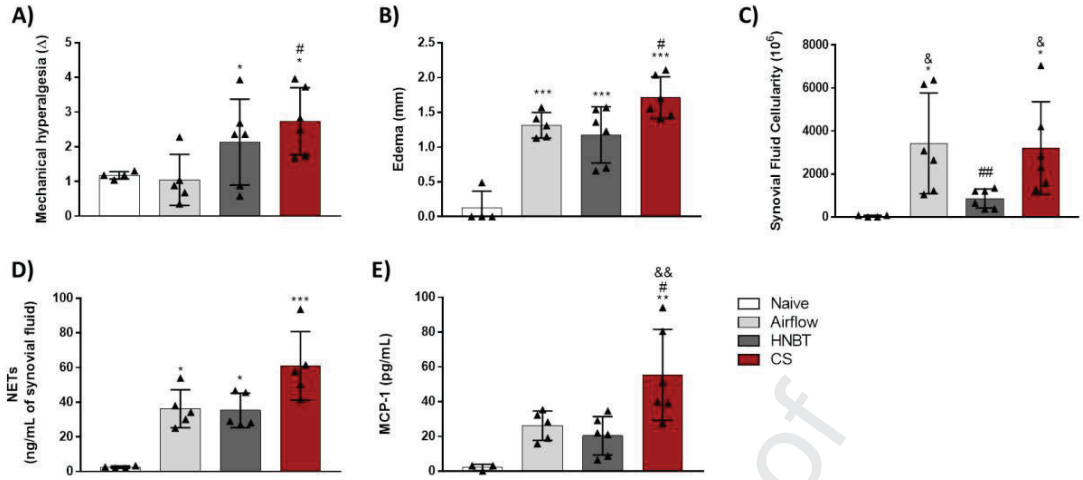

Figure 3

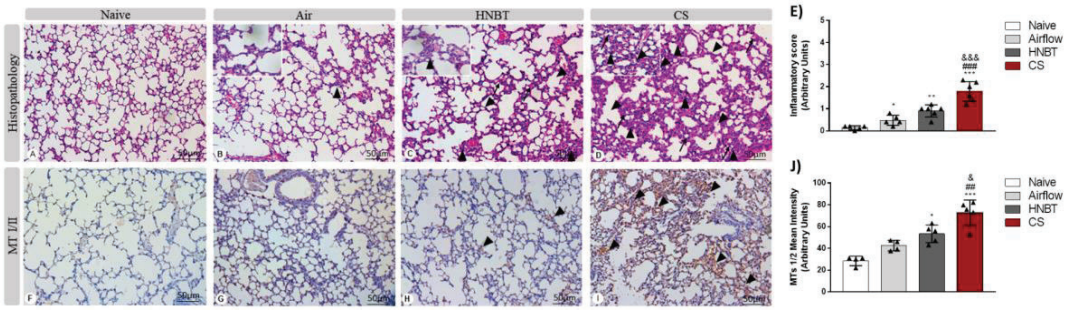

Figure 4

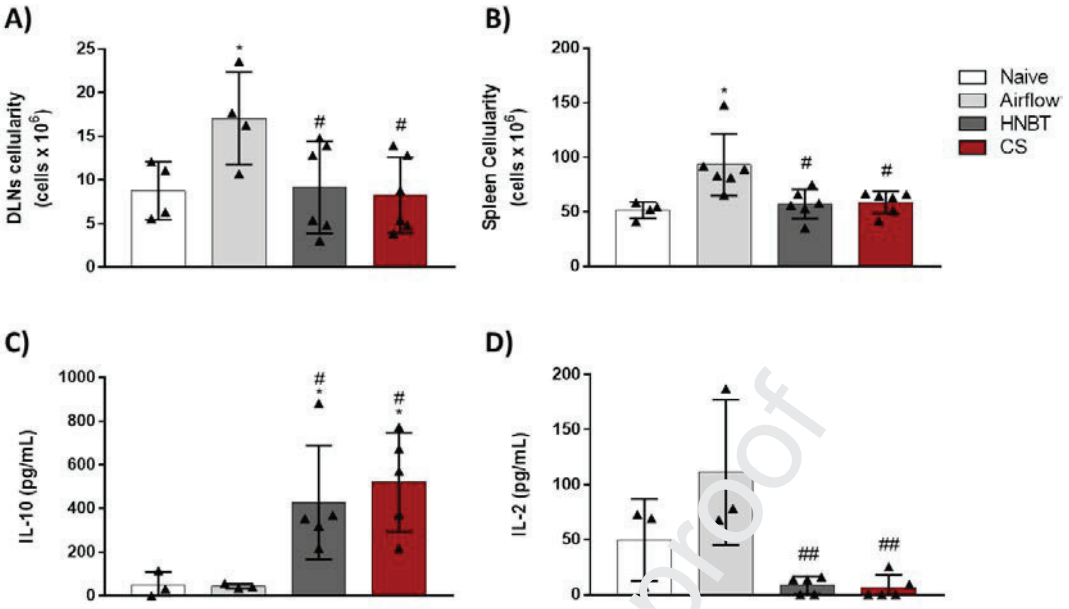

Figure 5

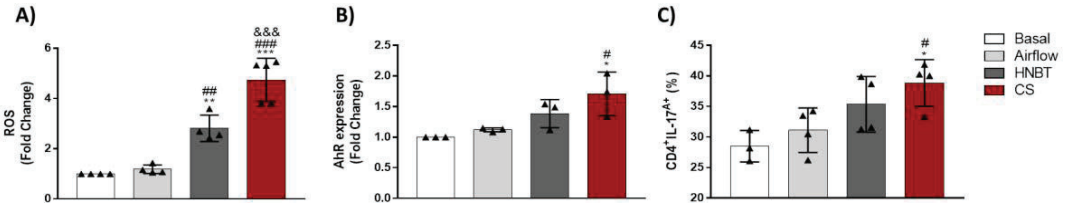

Figure 6

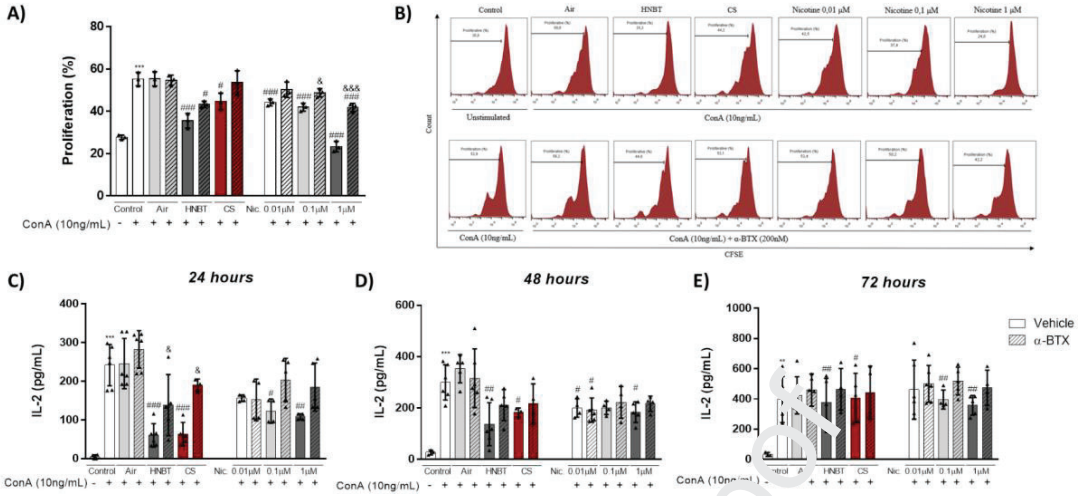

GRAPHICAL ABSTRACT

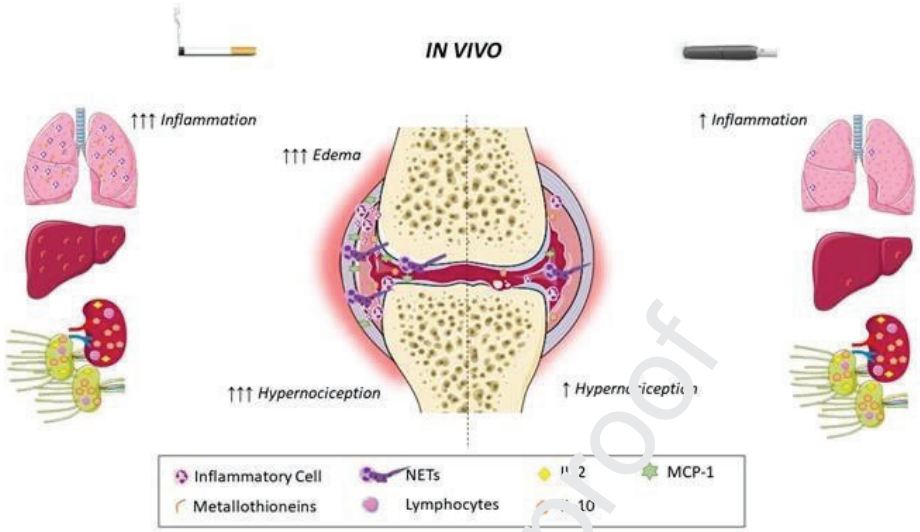

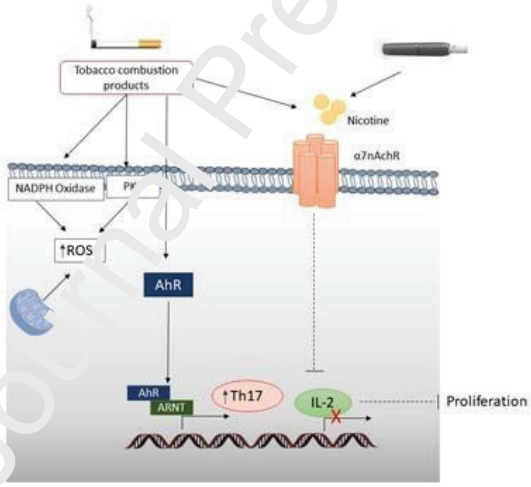

Highlights

- CS exposure worsens local and systemic AIA symptoms.
- CS exposure delivers metals and causes MTs expression in the inflamed lung during AIA.
- HNBT or CS exposures reduce lymphoid organs cellularity during AIA development.
- HNBT or CS exposures impair splenocyte proliferation and IL-2 secretion.
- Nicotine/α7nAchr mediates the impaired splenocyte functions caused by HNBT or CS exposures.